Optical detection and modulation at 2µm-2.5µm in silicon

D. J. Thomson,[1*] L. Shen,[1] J. J. Ackert,[2] E. Huante-Ceron,[2] A. P. Knights,[2] M. Nedeljkovic,[1] A. C. Peacock,[1] and G. Z. Mashanovich[1]

[1]*Optoelectronics Research Centre, University of Southampton, Southampton, SO17 1BJ, UK*
[2]*Department of Engineering Physics, McMaster University,1280Main Street West, Hamilton, L8S4L7, Canada*
**d.thomson@soton.ac.uk*

Abstract: Recently the 2µm wavelength region has emerged as an exciting prospect for the next generation of telecommunications. In this paper we experimentally characterise silicon based plasma dispersion effect optical modulation and defect based photodetection in the 2-2.5µm wavelength range. It is shown that the effectiveness of the plasma dispersion effect is dramatically increased in this wavelength window as compared to the traditional telecommunications wavelengths of 1.3µm and 1.55µm. Experimental results from the defect based photodetectors show that detection is achieved in the 2-2.5µm wavelength range, however the responsivity is reduced as the wavelength is increased away from 1.55µm.

OCIS codes: (130.4110) Modulators; (060.4080) Modulation; (040.5160) Photodetectors.

References and links

1. A. Narasimha, S. Abdalla, C. Bradbury, A. Clark, J. Clymore, J. Coyne, A. Dahl, S. Gloeckner, A. Gruenberg, D. Guckenberger, S. Gutierrez, M. Harrison, D. Kucharski, K. Leap, R. LeBlanc, Y. Liang, M. Mack, D. Martinez, G. Masini, A. Mekis, R. Menigoz, C. Ogden, M. Peterson, T. Pinguet, J. Redman, J. Rodriguez, S. Sahni, M. Sharp, T. J. Sleboda, D. Song, Y. Wang, B. Welch, J. Witzens, W. Xu, K. Yokoyama, and P. De Dobbelaere, "An ultra low power CMOS photonics technology platform for H/S optoelectronic transceivers at less than $1 per Gbps," *Proceedings of Optical Fibre Conference 2010 OMV4*, 1–3 (2010).
2. G. Z. Mashanovich, M. M. Milošević, M. Nedeljkovic, N. Owens, B. Xiong, E.-J. Teo, and Y. Hu, "Low loss silicon waveguides for the mid-infrared," Opt. Express **19**(8), 7112–7119 (2011).
3. R. Shankar, I. Bulu, and M. Lončar, "Integrated high-quality factor silicon-on-sapphire ring resonators for the mid-infrared," Appl. Phys. Lett. **102**(5), 051108 (2013).
4. Z. Cheng, X. Chen, C. Y. Wong, K. Xu, C. K. Fung, Y. M. Chen, and H. K. Tsang, "Focusing subwavelength grating coupler for mid-infrared suspended membrane waveguide," Opt. Lett. **37**(7), 1217–1219 (2012).
5. M. Nedeljkovic, A. Khokhar, Y. Hu, X. Chen, J. Soler Penades, S. Stankovic, D. J. Thomson, F. Y. Gardes, H. M. H. Chong, G. T. Reed, and G. Z. Mashanovich, "Silicon photonic devices and platforms for the mid-infrared," Opt. Mater. Express **3**(9), 1205–1214 (2013).
6. G. Roelkens, U. Dave, A. Gassenq, N. Hattasan, C. Hu, B. Kuyken, F. Leo, A. Malik, M. Muneeb, E. Ryckeboer, Z. Hens, R. Baets, Y. Shimura, F. Gencarelli, B. Vincent, R. Loo, J. Van Campenhout, L. Cerutti, J.-B. Rodriguez, E. Tournié, X. Chen, M. Nedeljkovic, G. Z. Mashanovich, L. Shen, N. Healy, A. C. Peacock, X. Liu, R. Osgood, and W. J. Green, "Silicon-based photonic integration beyond the telecommunication wavelength range," IEEE J. Sel. Top. Quantum Electron. **20**(4), 8201511 (2014).
7. M. Muneeb, X. Chen, P. Verheyen, G. Lepage, S. Pathak, E. Ryckeboer, A. Malik, B. Kuyken, M. Nedeljkovic, J. Van Campenhout, G. Z. Mashanovich, and G. Roelkens, "Demonstration of silicon-on-insulator mid-infrared spectrometers operating at 3.8 µm," Opt. Express **21**(10), 11659–11669 (2013).
8. Y. Hu, T. Li, D. J. Thomson, X. Chen, J. S. Penades, A. Z. Khokhar, C. J. Mitchell, G. T. Reed, and G. Z. Mashanovich, "Mid-infrared wavelength division (de)multiplexer using an interleaved angled multimode interferometer on the silicon-on-insulator platform," Opt. Lett. **39**(6), 1406–1409 (2014).
9. M. A. Van Camp, S. Assefa, D. M. Gill, T. Barwicz, S. M. Shank, P. M. Rice, T. Topuria, and W. M. J. Green, "Demonstration of electrooptic modulation at 2165nm using a silicon Mach-Zehnder interferometer," Opt. Express **20**(27), 28009–28016 (2012).
10. S. Zlatanovic, J. S. Park, S. Moro, J. M. C. Boggio, I. B. Divliansky, N. Alic, S. Mookherjea, and S. Radic, "Mid-infrared wavelength conversion in silicon waveguides using ultracompact telecom-band-derived pump source," Nat. Photonics **4**(8), 561–564 (2010).
11. *http://modegap.eu*

12. http://www.orc.soton.ac.uk/PHH
13. L. Vivien, A. Polzer, D. Marris-Morini, J. Osmond, J. M. Hartmann, P. Crozat, E. Cassan, C. Kopp, H. Zimmermann, and J.-M. Fédéli, "Zero-bias 40Gbit/s germanium waveguide photodetector on silicon," Opt. Express **20**(2), 1096–1101 (2012).
14. Z. Sheng, L. Liu, J. Brouckaert, S. He, and D. Van Thourhout, "InGaAs PIN photodetectors integrated on silicon-on-insulator waveguides," Opt. Express **18**(2), 1756–1761 (2010).
15. X. Wang, Z. Cheng, K. Xu, H. K. Tsang, and J. Xu, "High responsivity graphene/silicon heterostructure waveguide photodetectors," Nat. Photonics **7**(11), 888–891 (2013).
16. D. F. Logan, P. E. Jessop, and A. P. Knights, "Modeling defect enhanced detection at 1550 nm in integrated silicon waveguide photodetectors," J. Lightwave Technol. **27**(7), 930–937 (2009).
17. G. T. Reed, G. Z. Mashanovich, F. Y. Gardes, M. Nedeljkovic, D. J. Thomson, L. Ke, P. Wilson, S.-W. Chen, and S. H. Hsu, "Recent breakthroughs in carrier depletion based silicon optical modulators," Nanophotonics **0**(0), 1–18 (2013).
18. Y. Tang, J. D. Peters, and J. E. Bowers, "Over 67 GHz bandwidth hybrid silicon electroabsorption modulator with asymmetric segmented electrode for 1.3 µm transmission," Opt. Express **20**(10), 11529–11535 (2012).
19. D. Feng, S. Liao, H. Liang, J. Fong, B. Bijlani, R. Shafiiha, B. J. Luff, Y. Luo, J. Cunningham, A. V. Krishnamoorthy, and M. Asghari, "High speed GeSi electro-absorption modulator at 1550 nm wavelength on SOI waveguide," Opt. Express **20**(20), 22224–22232 (2012).
20. M. Liu, X. Yin, E. Ulin-Avila, B. Geng, T. Zentgraf, L. Ju, F. Wang, and X. Zhang, "A graphene-based broadband optical modulator," Nature **474**(7349), 64–67 (2011).
21. L. Alloatti, D. Korn, R. Palmer, D. Hillerkuss, J. Li, A. Barklund, R. Dinu, J. Wieland, M. Fournier, J. Fedeli, H. Yu, W. Bogaerts, P. Dumon, R. Baets, C. Koos, W. Freude, and J. Leuthold, "42.7 Gbit/s electro-optic modulator in silicon technology," Opt. Express **19**(12), 11841–11851 (2011).
22. M. Nedeljkovic, R. Soref, and G. Z. Mashanovich, "Free-carrier electro-refraction and electro-absorption modulation predictions for silicon over the 1-14 um wavelength range," IEEE Journal of Photonics **3**(6), 1171–1180 (2011).
23. M. W. Geis, S. J. Spector, M. E. Grein, R. T. Schulein, J. U. Yoon, D. M. Lennon, S. Deneault, F. Gan, F. X. Kaertner, and T. M. Lyszczarz, "CMOS-compatible all-Si high-speed waveguide photodiodes with high responsivity in near-infrared communication band," IEEE Photon. Technol. Lett. **19**(3), 152–154 (2007).
24. Y. Liu, C. W. Chow, W. Y. Cheung, and H. K. Tsang, "In-line channel power monitor based on helium ion implantation in silicon-on-insulator waveguides," IEEE Photon. Technol. Lett. **18**(17), 1882–1884 (2006).
25. B. Souhan, C. P. Chen, R. R. Grote, J. B. Driscoll, N. Ophir, K. Bergman, and R. M. Osgood, "Error-free operation of an all-silicon waveguide photodiode at 1.9 µm," IEEE Photon. Technol. Lett. **25**(21), 2031–2034 (2013).
26. H. K. Fan and A. K. Ramdas, "Infrared absorption and photoconductivity in irradiated silicon," J. Appl. Phys. **30**(8), 1127–1134 (1959).
27. J. J. Ackert, A. S. Karar, D. J. Paez, P. E. Jessop, J. C. Cartledge, and A. P. Knights, "10 Gbps silicon waveguide-integrated infrared avalanche photodiode," Opt. Express **21**(17), 19530–19537 (2013).
28. D. W. Zheng, B. T. Smith, and M. Asghari, "Improved efficiency Si-photonic attenuator," Opt. Express **16**(21), 16754–16765 (2008).
29. J. K. Doylend, A. P. Knights, B. J. Luff, R. Shafiiha, M. Asghari, and R. M. Gwilliam, "Modifying functionality of variable optical attenuator to signal monitoring through defect engineering," Electron. Lett. **46**(3), 234–235 (2010).
30. http://www.mellanox.com/

1. Introduction

Over the previous decade silicon has emerged as an attractive material in which to produce photonic integrated circuits and devices owing to its potential for low cost fabrication. The components required to realise a transceiver for a high speed data transmission link have been developed to the stage where commercial products based upon this technology have reached the market [1]. To date, most of the research into the individual components required for such a transceiver has been focused on the traditional telecommunication wavelength bands around 1.3µm and 1.55µm. Recently several groups have been exploring the use of silicon photonics into the mid-infrared (MIR) (2-20µm). There have been reports on low loss waveguides in different material platforms [2–4], efficient couplers and splitters [5, 6], multiplexers [7, 8], hybrid lasers and detectors [6], modulators [9], and nonlinear effects [10]. The wavelengths beyond 3µm, and particularly those beyond 8µm where many molecules exhibit strong absorption (i.e., the 'fingerprint' region), are interesting for sensing applications. However, fewer group IV devices have been demonstrated in this wavelength range due to the more challenging fabrication, arising from a need to use different material platforms, and the unavailability of suitable testing equipment. Research in the short-wave infrared (2-3μm) wavelength range, on the other hand, has been quite dynamic as many techniques and equipment available for telecom applications can be used in this region. This wavelength region has also emerged as a strong contender for the next generation of communication systems. Traffic on the global communications infrastructure continues to increase 50% year-on-year, driven by rapidly expanding and increasingly demanding applications, as well as the emergence of new concepts such as cloud computing and telesurgery. With continued steep growth in transmitted data volumes on all media, there is a widely-recognised and urgent need for more sophisticated photonics technologies in both the core and access networks to forestall a 'capacity crunch'. One promising solution is to use new spectral bands in the short-wave region for optical communication systems and the investigation of new glasses and optical fibres, amplifiers and regenerators, and nonlinear processing up to 3μm, is currently underway [11, 12]. In order to unlock the cost benefits of silicon photonics in these wavelength bands the different transceiver components need to be redeveloped. Two key components in a photonic transceiver are the high speed photodetector and high speed optical modulator. In the near-infrared (NIR) the most popular technique to form high speed photodetectors in silicon has been to introduce germanium to the wafer surface [13]; however, this method is not suitable for the 2-3μm wavelength range as germanium is largely transparent. Alternative methods that can be extended beyond 2μm include III-V on silicon detectors [14], graphene on silicon [15], and defect based detectors [16], where the latter approaches have the advantage of CMOS compatibility. In terms of modulation, high speed optical modulators in the NIR have typically made use of the plasma dispersion effect [17], although approaches based upon the hybridisation of other materials such as III-V [18], germanium [19], graphene [20] and polymers [21] have also been successfully demonstrated. However, to date, little work has been done to achieve optical modulation in the 2–3μm band [9, 22]. In this paper we analyse the performance of both defect based detectors and a plasma dispersion effect modulator fabricated from commercially available variable optical attenuators (VOA) in the 2–2.5μm wavelength band. Experimental results from the modulator show that the plasma dispersion effect becomes much more effective in the 2–2.5μm wavelength range as compared to 1.3μm and 1.55μm. Photodetection is achieved in the 2–2.5μm wavelength band, however, the responsivity of the devices becomes gradually reduced as the wavelength is increased from the 1.55μm.

2. Photodetection

Devices which utilize defect mediated absorption have been established for some time as a viable method for the development of monolithic waveguide photodetectors suitable for use in the *C* and *L* bands (for example see [16, 23, 24]). The introduction of defect states within the bandgap permit the absorption of sub-bandgap photons through a mechanism of optical absorption and thermal excitation from the defect state [16]. With optimisation of the defect concentration responsivities approaching 1A/W, bandwidths in excess of 30GHz are possible. While characterisation up to wavelengths of 1.9μm has been demonstrated [25], albeit with a 3-5dB decrease in responsivity compared with detection at 1.55μm, no attempt has been made to assess the potential for these detectors in the extended MIR range. Experimental evidence for defect mediated absorption in irradiated silicon up to wavelengths of 3μm was demonstrated as early as 1959 by Fan and Ramdas [26]. A simple interpretation of the data from [26] would suggest that for geometrically equivalent waveguide detectors (ignoring the impact of mode size change with varying wavelength) one might expect a decrease in responsivity of around 3dB for 2μm and perhaps as much as 10-20dB for 2.5μm when compared to that for a 1.55μm wavelength. Even with this decrease in sensitivity, there is a significant attraction for using these types of detectors in optical links using extended wavelengths. Indeed, in light of the recent demonstration of avalanche detection for a

#208941 - $15.00 USD Received 26 Mar 2014; revised 14 Apr 2014; accepted 16 Apr 2014; published 28 Apr 2014

wavelength of 1.55µm [27], we may reasonably expect a DC responsivity >1A/W for the 2–2.5µm range for a device with an optimised geometry and bias.

The photodetectors used in this study were modified from a commercial VOA originally made available by Kotura Inc. The fabrication details and performance of these devices when functioning as either VOAs or tap detectors for use at 1550nm may be found elsewhere [28, 29]. Following the processing to form the VOA (including metal/dielectric deposition) three devices were implanted with boron ions to a dose of $1x10^{12}$, $5x10^{12}$ or $1x10^{13}cm^{-2}$; at an energy of 4MeV. All devices were subsequently annealed at 200°C for 5 minutes in a nitrogen ambient. The detectors were characterised around 1.55µm and between 2µm and 2.5µm. At 1.55µm light from a tunable laser is passed to a collimating lens via an optical fibre. The collimated light is then passed through free-space to a second lens which focuses the light on to the input facet of the optical waveguide. In the case of the 2–2.5µm wavelengths, collimated light is passed directly from the laser to a lens which focuses the light on to input waveguide. At the output side of the detector chip the light is collected from the waveguide facet using a further lens which collimates the light, which is then passed through free-space to a commercial detector. The electrode pads of the devices were contacted using probes that were connected to a picoammeter, allowing application of the reverse bias and measurement of the resultant photocurrent. A schematic of the experimental set-up together with the device layout is shown in Fig. 1 (a).

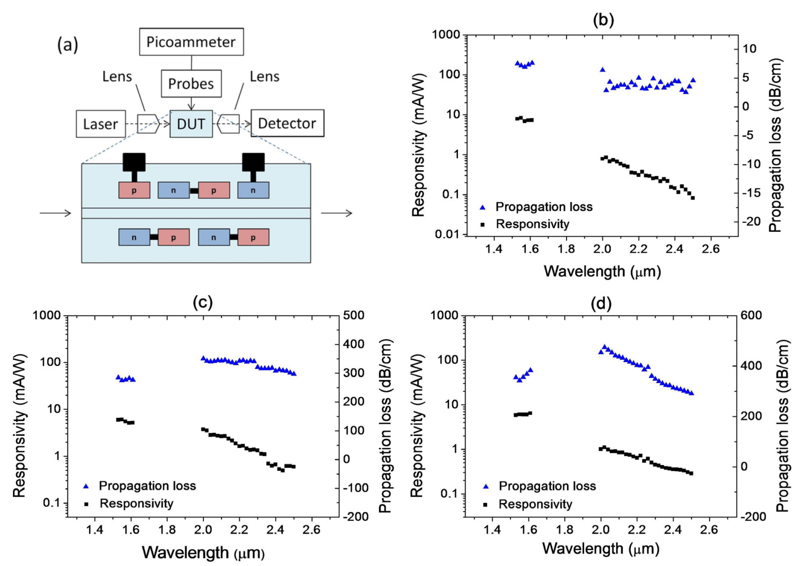

Fig. 1. Schematic of setup with device layout (a). Responsivity versus wavelength for the detector with boron implantation dose of (b) $1x10^{12}.cm^{-2}$, (c) $5x10^{12}.cm^{-2}$, and (d) $1x10^{13}.cm^{-2}$.

The length of the entire fabricated chip was 17mm, and comprised of a ~5mm photodetector section positioned in the centre with ~6mm of passive waveguide on both the input and output sides. The ion implantation process which was used to create the defects was not masked and therefore the entire length of the waveguide was implanted. This means that the optical power reaching the detector is subject to the optical losses in the input section as well as coupling and lens losses. The lens loss was characterised separately and the coupling loss estimated to be approximately 1.6dB per facet. The coupling loss is dominated by reflection losses since the waveguide cross section is relatively large for these devices. The propagation loss at each wavelength was then calculated from the measurements of the input and output powers and the losses in the system. The power at the input of the

#208941 - $15.00 USD Received 26 Mar 2014; revised 14 Apr 2014; accepted 16 Apr 2014; published 28 Apr 2014

photodetector section was then calculated in each case in order to obtain the detector responsivity.

Figure 1(b), 1(c) and 1(d) show the optical detection and propagation losses in the wavelength range of 1.53-1.61µm and 2–2.5µm for the three photodetectors with different implantation doses. The difference in trend in propagation loss between samples is likely to be due to differences in the implantation conditions [26]. For the best performing device (i.e., that implanted to a dose of $5x10^{12}cm^{-2}$), the responsivity at 2500nm is reduced by a factor of 10 compared to 1550nm; while for 2000nm the responsivity is approximately 80% of that for 1550nm. The absolute values of responsivity are modest, as one would expect for such large waveguides (4.7µm height, 3.5µm width and 3.1µm slab height), with the results being consistent with those reported by Doylend et al. [29]. These results are in fact extremely encouraging and suggest that small cross-section detectors (currently being designed by the authors) should provide responsivities >1A/W, and bandwidths of 10Gbps when operated in the avalanche regime [27]. The trend for responsivity as a function of implantation dose for these types of detectors is dominated by a trade-off between increasing absorption with increasing dose (and defect concentration), and a degradation in diode electrical characteristics as the dose is increased (a result of carrier recombination). The absolute values of responsivity are however dependent upon the waveguide geometry and ion species, energy and dose. Quantitative discussion of these issues was provided in [16]. It would appear that for the current detector geometries and for the ion species chosen (i.e. boron) the range of 10^{12} to $10^{13}cm^{-2}$ would bracket the optimum dose. We show evidence of this conclusion in the fact that of our three doses, $5x10^{12}cm^{-2}$ produces the greatest amount of responsivity (although we cannot be sure that this is the optimum dose). High speed operation of these photodetectors is not expected due to the large waveguides used. Scaling this type of device to sub-micrometer size waveguides can yield speeds of 10Gbps as shown in [27].

3. Modulation

Plasma dispersion effect modulators based upon the injection, depletion and accumulation of free electrons and holes have been widely demonstrated in silicon. The attraction of the plasma dispersion effect is the combination of CMOS compatibility, achievable performance and fabrication simplicity. At 1.3µm and 1.55µm a large number of plasma dispersion effect modulators have been demonstrated with impressive results [17]. To date there has been very little work on plasma dispersion effect modulators at MIR wavelengths, although a theoretical analysis [22] and one experimental demonstration at 2.165µm [9] have been published. The theory of [22] suggests that as the wavelength is increased, the change in refractive index and absorption achieved for a given change in free carrier density is enhanced. Here we experimentally analyse the relative effectiveness of a carrier injection based VOA at 1.3µm, 1.5µm, 2µm and 2.5µm. The same VOA structure as used for the photodetectors in the previous section is employed, however in this case post-process implantation of boron ions was not performed. The devices therefore consist of a *p-i-n* diode with the waveguide formed in the intrinsic region, which in this case is largely defect free and therefore the losses in this case are lower than in the case of the photodetectors (~1dB/cm [30]). When the device is forward biased, free carriers are injected into the intrinsic waveguide region and cause an increase in the absorption of the propagating light.

The optical output was measured for varying forward bias voltages and injection currents, using the same experimental setup as was used for the photodetector measurements. The optical transmission is plotted against current in Fig. 2 for the four different wavelengths. The results are normalised to the transmission with no bias applied. The reduction in transmission is due to the presence of injected free carriers in the waveguide. The slight ripple in the curves is due to the waveguide acting as a Fabry-Perot cavity and changes in the

#208941 - $15.00 USD Received 26 Mar 2014; revised 14 Apr 2014; accepted 16 Apr 2014; published 28 Apr 2014

refractive index due to the injected carriers. Ideally we would compare our experimental results with the theoretical analysis of [22]. However, calculations based on the analysis suggest that the free carrier densities achieved over the injection currents used in this work are approximately $1x10^{17}cm^{-3}$, which is out of the range of the minimum densities used to develop the expressions in [22] ($3.2x10^{17}cm^{-3}$ and $5x10^{17}cm^{-3}$ for electrons and holes, respectively). According to the theory, with an injected electron and hole density of $1x10^{17}cm^{-3}$ the attenuation in dB achieved at 1.55µm, 2µm and 2.5µm is 1.7, 2.9 and 3.7 times more than the attenuation at 1.3µm, whereas according to the experimental results of Fig. 2 it is 2.2, 4.5 and 6.3 times more, respectively. Thus we cannot be confident that fitting of the attenuation curves of Fig. 2 with this theory will provide a meaningful interpretation of the results for all four wavelengths.

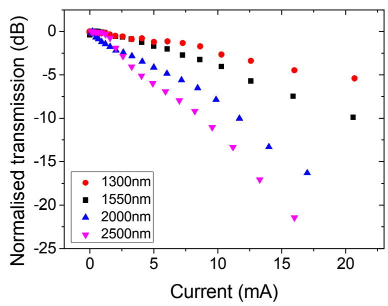

Fig. 2. Normalised transmission versus drive current at 1.31µm, 1.55µm, 2µm and 2.5µm.

The curves of Fig. 2 do, however confirm that as the wavelength is increased the plasma dispersion effect becomes more effective. These results suggest that plasma dispersion effect modulators used for the 2µm wavelength window could be much more compact and/or require a much lower drive voltage (and therefore lower power consumption) than at the traditional NIR telecommunication wavelength bands. The speed of the device used in this analysis is slow due to the large size of the waveguide and the use of carrier injection [28]. By scaling to a smaller waveguide and by using carrier depletion or accumulation techniques, operation at speeds up to 40Gbit/s and beyond can be expected as shown in the NIR [17].

4. Conclusion

Silicon photonic based defect photodetectors and a plasma dispersion effect modulator have been characterised in the 2–2.5µm wavelength band. For the detectors it is shown that operation is possible in this wavelength range, however, the responsivity is reduced as compared to 1.55µm. The results from the optical modulator shows that a large increase in the effectiveness of the plasma dispersion effect is achieved as the wavelength is increased from the traditional telecommunication windows of 1.3µm and 1.55µm to the 2–2.5µm range. These encouraging results show that silicon photonics has bright prospects for the implementation of integrated photonic circuits in this newly proposed short-wave band for extended telecommunications applications.

Acknowledgments

The research leading to these results has received funding from the EPSRC in the UK to support the MIGRATION and Silicon Photonics for Future Systems projects; and NSERC in Canada. Goran Mashanovich acknowledges support from the Royal Society through his Royal Society Research Fellowship. We thank members of the Kotura silicon photonics team for supplying the VOA chips.